Deep–Sea Research Part II 143 (2017) 62–72

Contents lists available at ScienceDirect

Deep–Sea Research II

journal homepage: www.elsevier.com/locate/dsr2

Flux and stable C and N isotope composition of sinking particles in the Ulleung Basin of the East/Japan Sea

Jung Hyun Kwak[a,1], Eunah Han[a,1], Jeomshik Hwang[b], Young II Kim[c], Chung Il Lee[d], Chang-Keun Kang[a,*]

[a] School of Earth Sciences and Environmental Engineering, Gwangju Institute of Science and Technology, Gwangju 61005, Republic of Korea
[b] School of Earth and Environmental Sciences, Seoul National University, Seoul 08826, Republic of Korea
[c] East Sea Research Institute, Korea Institute of Ocean Science & Technology, Gyeongbuk 36315, Republic of Korea
[d] Department of Marine Bioscience, Gangneung-Wonju National University, Gangneung 25457, Republic of Korea

ARTICLE INFO

Keywords:
Sediment traps
Sinking particles
Particulate Flux
Particulate organic carbon
Isotopes
Ulleung Basin

ABSTRACT

Seasonal variability of sinking fluxes of total mass (TMF), particulate organic carbon and nitrogen (POC and PON) was examined using sinking particles collected from sediment traps during July 2011 to December 2011, and December 2012 to June 2013 at an offshore channel site; and from November 2013 to August 2014 at a nearshore slope site of the Ulleung Basin in the East/Japan Sea. $\delta^{13}C$ and $\delta^{15}N$ values of sinking particles were measured to elucidate the major export processes of POC and PON. Annual TMF (112–638 g m^{-2} yr^{-1}) and fluxes of POC and PON (9.6–32.1 g C m^{-2} yr^{-1} and 1.2–4.5 g N m^{-2} yr^{-1}, respectively) in the Ulleung Basin corresponded to the upper limit of values reported for other open seas and oceans in the world. No great seasonal variability in both quantitative (TMF, and fluxes and contents of POC and PON) and qualitative (C/N ratios, and $\delta^{13}C$ and $\delta^{15}N$ values) estimates of vertical fluxes was observed, reflecting a steady standing stock of chlorophyll *a* in the upper part of water column. Furthermore, high contents of POC and PON and nearly constant $\delta^{13}C$ and $\delta^{15}N$ values in sinking particles collected in the sediment traps, indicate that primary production in the euphotic zone may be a good predictor of TMF and export flux of organic matter. In this regard, our pilot study points out the importance of high annual primary production and low water temperature (< 1 °C) beneath the 200-m water depth, which would enable more sinking particles to be preserved during export process by limiting microbial decomposition activity in the water column, in determining the high annual flux of sinking particles in the Ulleung Basin (UB). A simple stable isotope mixing model of sinking particles indicates that despite a slight seasonal variation, the contribution of intact phytoplankton to sinking organic flux is significant to the POC and PON flux in the UB. Further continuous time series sediment trap experiments are proposed to estimate the contribution of allochthonus sources such as lateral advection through resuspended clay mineral, and aeolian and terrestrial inputs to the sedimentary flux.

1. Introduction

The biological carbon pump describes material flow across multiple depth layers of the ocean from the euphotic zone to the dark benthic zone (Volk and Hoffert, 1985). The pump operates in several stages, namely production, export, flux to depth, and sedimentation processes, and the efficiencies of the individual processes are closely interrelated (Deuser et al., 1981, 1983; Karl et al., 1996; Thunell, 1998). Eppley and Peterson (1979) demonstrated that the export flux of particulate organic carbon (POC) is balanced by new production that is fueled by allochthonous nitrogen, clarifying how primary production controls the export flux. In fact, the export flux of POC is proportional to the total mass flux (TMF) across the boundary between the euphotic and bathypelagic zones (Broecker, 1974). According to variations in the primary production and biological processes, the contribution of the export flux to the TMF varied up to 30% across the various regions of the world ocean (Honjo et al., 2008 and references therein). Therefore, the physical and biogeochemical dynamics affecting the primary production, such as stratification and nitrogen availability in the euphotic zone, are important in determining the POC export flux of a specific region.

The primary production in the euphotic zone also regulates the major pathway of POC export (Ducklow et al., 2001). Sinking particles

* Corresponding author.
E-mail address: ckkang@gist.ac.kr (C.-K. Kang).
[1] JHK and EH equally contributed to this paper.

http://dx.doi.org/10.1016/j.dsr2.2017.03.014
Received 29 February 2016; Received in revised form 5 October 2016; Accepted 27 March 2017
Available online 04 April 2017
0967-0645/

are in the form of either intact phytoplankton aggregates with biogenic mineral ballasts, such as biogenic silica and calcium carbonates, or repackaged mesozooplankton fecal pellets (Osterbereg et al., 1963; McCave, 1975). The relative importance of each form of sinking particles appears to be related to primary production in the euphotic zone. Trap samples collected in the eutrophic coasts or in the upwelling zones, where the primary production is high, usually include the large proportion of intact phytoplankton aggregates (Smetacek et al., 1976; Staresinic et al., 1978; Iversen et al., 2010). The seasonal variation in the proportion of intact phytoplankton aggregates in the TMF synchronizes with that of the sea surface blooms of phytoplankton taxa that form biogenic ballasts (Deuser, 1986; Mohiuddin et al., 2004). In contrast, sediment trap samples of oligotrophic regions with a high mesozooplankton biomass have been reported to contain higher portion of mesozooplankton fecal pellets than those of high primary production regions, accounting for up to one-tenth of TMF (Turner, 2002; Laurenceau-Cornec et al., 2015). Thus, the relative proportion of phytoplankton aggregates to mesozooplankton fecal pellets in sediment trap samples can be an indicator for high primary production in the upper layer and consequent high export flux.

The East/Japan Sea (EJS) is surrounded by Korea, Russia, and Japan, and is connected to the Pacific Ocean through four shallow (< 140 m) straits. It can be characterized as a Mediterranean-type miniature ocean because of its own thermohaline circulation, which resembles the ventilation of the North Atlantic (Kim et al., 2001). Therefore, knowledge of the biogeochemical processes in the EJS can allow us to better understand the biological pump of the world ocean (Talley et al., 2006). The Ulleung Basin (UB) is a highly productive oceanic basin in the southwestern part of the EJS (Yamada et al., 2005; Ashjian et al., 2006; Lee et al., 2009). The Tsushima Warm Current, which branches off from the nutrient-poor Kuroshio, prevails in the surface water of the UB, and the deep water (> 2000 m) is exchanged through the Ulleung interplain gap. Despite the penetration of warm and nutrient-depleted surface water in the UB, the primary production in the UB is comparable to that of the ocean's upwelling regions (Kwak et al., 2013a; Joo et al., 2014). This high productivity is explained by coastal upwelling (Hyun et al., 2009; Yoo and Park., 2009) and a shallow nutricline depth, leading to a large supply of nutrients to the euphotic zone as indicated by a high *f*-ratio (the ratio of nitrate-based production to total primary production) during summer (Kwak et al., 2013b, 2014). The primary production in the surface layer of the UB is high during the spring and the fall whereas it is low during the summer. However, the depth-integrated primary production is consistent from the spring to the fall. This can be explained by the formation of the subsurface chlorophyll maximum in the UB during the summer, which results from the shoaling nitracline (Kwak et al., 2013b, 2014). Because this high primary production of the UB is likely to result in a high export flux, there have been several studies estimating the sinking POC flux in the UB. Sediment trap investigations revealed an annual average POC flux of 19.0 mg C m^{-2} d^{-1} in the UB, which was higher than that in oligotrophic regions (Hong et al., 1997a, 1997b, 2008). The indirect approaches to estimating the sinking POC flux of the UB using $^{234}Th/^{238}U$ disequilibrium models and He isotopes suggested a potentially high new primary production in the summer in the UB, with an effect on the POC export flux (Hahm and Kim, 2001; Kim et al., 2011). Nevertheless, the effect of high primary production on the seasonality of the POC flux and its export pathway in the UB remains speculative because of a lack of in situ measurements of the POC flux or biogeochemical analysis of the sinking particles.

Although the high annual primary production and its seasonal pattern in the upper layer of the UB has been reported, the potential effect of high primary production on the POM export flux has not been examined. In the present study, we aimed to report the annual POM export flux in the UB using a time-series sediment trap analysis. We hypothesized that the annual POM flux of the UB would be high compared with the values previously reported in other ocean regions due to high primary production. To test this hypothesis, we estimated the TMF and the fluxes of POC and PON and compared them with the data obtained from previously reported deep-sea sediment traps at various locations in the EJS (see Appendix 5). Chlorophyll *a*, physical factors, and nitrate concentration in the overlying water column were measured to investigate seasonal variations in the biogeochemistry of the euphotic zone with those in particle sinking patterns. The POM export flux of the summer in the UB was compared with that of the spring and the fall to determine if the formation of the subsurface chlorophyll *a* maximum in the summer contributes significantly to the POM export flux to the UB. The seasonal and spatial variations of the C/N ratio and C and N stable isotope values of the sinking particles were analyzed to identify if the sinking particles were mainly derived from the primary production in the upper layer of the UB. A stable isotope mixing model, which calculated the relative importance of the intact phytoplankton aggregates to mesopelagic zooplankton fecal pellets, was used to confirm whether the stable isotope values of the sinking particles in the UB were consistent with the properties of the eutrophic ocean with high primary production.

2. Materials and methods

2.1. Sediment-trap sample collection and ancillary measurements

To compare the sinking processes of organic particles between the continental slope and deep-sea floor in the UB, two sites were chosen for the deployment of sediment traps, one offshore (37°38.1′ N, 131°20.6′ E; 2200 m water depth) and another in the nearshore (36°31.9′ N, 130°0.0′ E; 850 m water depth) (Fig. 1). In the offshore channel site, sediment traps were deployed by the R/V Onnuri on July 4, 2011 and recovered one year after deployment. Another series of traps were deployed in July 2012 and recovered on June 27, 2013. For two successive deployment years, we successfully obtained trapped materials over a six-month interval: July 4, 2011 to December 19, 2011 and December 01, 2012 to June 27, 2013. In the nearshore slope site, sediment traps were deployed by the R/V Tamsa 2 on November 12, 2013 and recovered in October 2014. Because we failed to obtain trapped materials at the end of the deployment, we used data from November 12, 2013 to August 19, 2014 in this study. At the offshore site, samples of sinking particles were collected at three depth layers (500, 1000, and 2000 m) using time-series sediment traps (SMD26S-6000, Nichiyu Giken Kogyo Co. Ltd., Kawagoe, Japan). These sediment traps were of conical type with an aperture diameter of 80 cm and a height-to-diameter ratio of 1.32, and consisted of 26 receiving cups turning at eight-day intervals. At the nearshore site, sediment traps of the same type were deployed at water depths of 700 and 800 m and the sampling interval of each cup was programmed to 14 days. Before deployment, the sampling cups of the traps were filled with artificial seawater containing 35 g NaCl and saturated $HgCl_2$ solution as a preservative (final concentration, 5%). After the recovery of the traps, the collected samples were stored at 4 °C until laboratory analyses.

To investigate the temporal variation in the water column structure in the upper layer at the nearshore site, temperature, salinity, and density were observed from December 2012 using a moored buoy system equipped with eight CTD sensors (water depths of 0, 10, 20, 30, 50, 75, 100, and 200 m). Additional onboard CTD (SBE 911 Plus, Seabird Electronics Inc., Bellevue, USA) measurements and water collection were seasonally conducted at both the offshore and nearshore sites (February, May, August, and November) to characterize the water column conditions such as stability, nutritional condition, and phytoplankton biomass. Water samples were collected to measure nitrate and chlorophyll *a* concentrations at seven depths (0, 10, 20, 30, 50, 75, and 100 m) using a rosette sampler combined with CTD sensors.

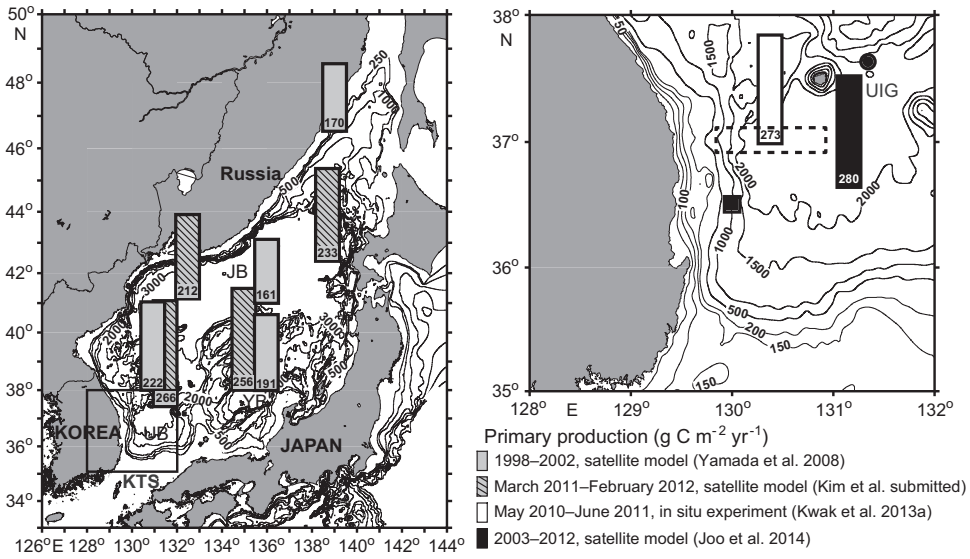

Fig. 1. Map of the East/Japan Sea with the annual primary production of each region and the locations of the offshore (circle) and nearshore (rectangle) mooring sites, in the Ulleung Basin (UB).

2.2. Laboratory analyses

Whole sinking materials collected in the sampling cups of the traps were split using a wet sample divider (McLane Research Laboratories, WSD-10). A tenth of each sample was rinsed three times with Milli-Q water and filtered with 1 mm nylon mesh to remove any large particles such as swimming and planktonic organisms. These subsamples were lyophilized. The dried samples were weighed for gravimetric determination of the TMF. The other subsamples were homogenized by pulverizing and were stored at −70 °C until later analyses.

For water column variables, nitrate was measured by standard spectrophotometric methods (Parsons et al., 1984) and the chlorophyll *a* concentration was determined after filtration of 1 l of water onto Whatman GF/F filters. The filters were extracted with 90% acetone in dark and cool (4 °C) conditions overnight, and then an aliquot of acetone extract was analyzed using a fluorometer (Turner Designs, Sunnyvale, CA, USA).

The C and N stable isotope ratios of the sinking particles were analyzed to assess the spatial and temporal variations in the major sources of organic matter, making comparisons with intact phytoplankton aggregates and mesozooplankton fecal pellets collected in the upper water column. Powdered samples for stable isotope ratios were fumed with concentrated HCl for 24 h and then transferred to tin capsules. The samples were analyzed on a continuous-flow isotope-ratio mass spectrometer (CF-IRMS; Isoprime 100; IsoPrime Ltd, Cheadle Hulme, UK) connected to an elemental analyzer (Vario MICRO Cube; Elementar Analysensysteme GmbH, Hanau, Germany). The samples were placed in the elemental analyzer to oxidize at high temperature (1150 °C) before the determination of the C and N contents and concentrations of solid samples. Furthermore, the resultant CO_2 and N_2 gases were introduced into the CF-IRMS using He carrier gas. The isotopic data are expressed using the delta (δ) notation to represent the relative difference between the isotope ratios of the sample and conventional standards (i.e. Pee Dee Belemnite for C and atmospheric air for N), using the equation: $\delta X\ (‰)=[(R_{sample}/R_{standard})-1]\times 10^3$, where X is ^{13}C or ^{15}N and R is the $^{13}C/^{12}C$ or $^{15}N/^{14}N$ ratio. The stable isotope abundances were calibrated by international standards as reference materials [8542 ANU, $\delta^{13}C=-10.47\pm0.13‰$, National Institute of Standards and Technology (NIST), Gaithersburg, MD, USA; RM 8568 UG, $\delta^{15}N=-1.8\pm0.1‰$, NIST]. Secondary standards of known relations to the international standard were used as reference materials and analyzed with every 10th unknown sample. The analytical precisions of the repeated measurements of internal peptone and urea standards were within 0.15‰ for $\delta^{13}C$ and 0.20‰ for $\delta^{15}N$, respectively.

2.3. Data analysis

Fluxes of POC and PON were calculated from the TMF and from their content (%) in sinking particles. The annual TMF and annual POC and PON fluxes (g m^{-2} yr^{-1}) were estimated by averaging the interpolated daily fluxes.

Statistical hypothesis tests were applied to analyze between-depth differences in quantitative (TMF, and fluxes and contents of POC and PON) and qualitative (C/N ratios, and $\delta^{13}C$ and $\delta^{15}N$ values) estimates of sinking particles. This was primarily based on nonparametric tests because none of the estimates conformed to a normal distribution even after transformation. The Kruskal–Wallis test was used to determine whether the estimates differed between the three trap deployment depths at the offshore site. When the difference was significant, the Mann–Whitney *U* test was used for the three pairs of depths and for the data from the nearshore site. Potential interactions between eight qualitative and quantitative estimates [140 cases = $_8C_2$ (interaction between two estimates among eight)×5 depths (3 and 2 at the offshore and nearshore sites, respectively)] were checked by using Spearman's rank correlation coefficients to support causal relationships between the fluxes and the major sources of organic matter. Linear statistics and correlation analysis were performed using SPSS 12.0.1 (IBM SPSS Statistics, Armonk, NY).

Circular statistics were applied to analyze the changing patterns of all estimates with time. The polar plots compare seasonal patterns estimated between the sampling depths (Fig. 8). In the polar plot, a data point far from the center of the plot indicates a higher value of an estimate at the date corresponding to the clockwise angle of the point. The circular statistical approach was conducive to identifying changing patterns at short time-scales (i.e. nearly fortnightly at the nearshore site and weekly at the offshore site). Moore's modified Rayleigh test was used to check the uni- and bimodalities of the temporal distribution. This is a nonparametric second-order test that weights the mean angles with the rank order of the magnitude of each vector to determine whether the mean vectors are randomly (uniformly) distributed around a circle (Zar, 1998). The alternative hypothesis for this test was that peaks of an estimate were concentrated in a specific period (i.e. unimodality) or two periods with an approximately six-month gap

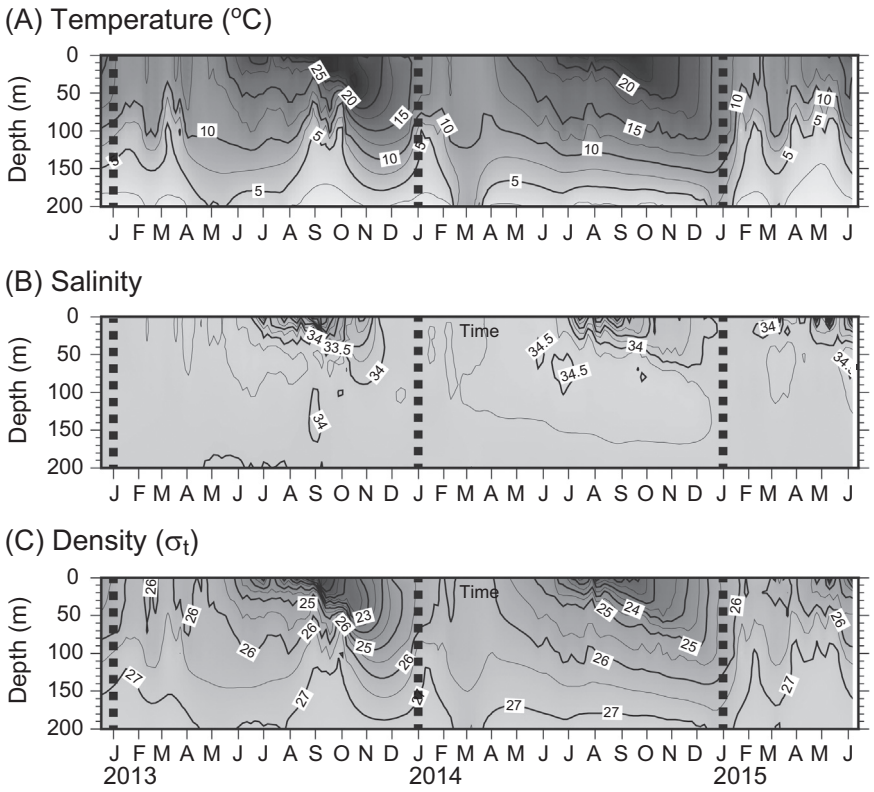

Fig. 2. Temperature (°C), salinity, and density (σ_t) time series in the upper 200 m observed using the mooring buoy system at the nearshore site, from December 2012 to June 2015.

(i.e. bimodality) throughout the year. When a distribution of an estimate was significant ($P < 0.01$), an ellipse of the weighted mean vector standard deviation was presented on the polar plot to show the directionality of the distribution with the position of its centroid and the direction of its major axis. Prior to statistical tests, the data were scaled to the range 0–1, and pairs comprising a date and the corresponding value of an estimate were divided into subgroups and defined as a vector. The angle of the vector for a given date in a year was doubled and reduced to a 0° to 360° range for the bimodality test. Circular statistical analyses were conducted using the Oriana 4.0.2 software (Kovach Computing Service, Anglesey, UK; Kovach, 1994). For all statistical analyses, the significance level was set to $P < 0.05$.

3. Results

3.1. Water column characteristics

The vertical patterns of temperature, salinity, and density (σ_t) continuously measured by the mooring buoy system at the nearshore slope site were characterized by two distinct seasonal features (Fig. 2). The water column was vertically well mixed during the winter-to-spring period (December–May). Because of the high temperature and low salinity of the surface water, the water column was strongly stratified during the summer-to-fall period (June–November). A similar seasonal distinction was also observed at the offshore site (Fig. 3A). The cold-water mass (< 5 °C) was maintained beneath the 300-m water depth throughout the year. The nitrate concentration of surface water varied from oligotrophic in August and November to eutrophic in February and May, coinciding with a deepening of the surface mixed layer that resulted from the change in water column stability. The nitrate concentration was homogenized within the 75-m depth during the well-mixed season (Fig. 3B). The nitrate in the surface water began to be depleted in May when the water column became stable, and then a nitracline began to develop at both sites. The nitrate concentration decreased (< 0.5 μM) in the upper 25 m water depth in August when the water column was strongly stratified and the nitracline shoaled. The chlorophyll *a* concentration and its vertical distribution patterns were similar between the offshore and nearshore sites (Fig. 3C). The chlorophyll *a* concentration of the surface water was highest in May (0.39–0.47 μg l^{-1}) and lowest in August (0.02–0.03 μg l^{-1}). Although the concentration of surface chlorophyll *a* in August was an order of magnitude lower than in November or February (0.10–0.27 μg l^{-1}), the standing stock of chlorophyll *a* integrated from the surface to a depth of 100 m was higher in August (21.9–27.5 mg m^{-2}) than in November (14.4–20.7 mg m^{-2}) or February (16.3–17.1 mg m^{-2}).

3.2. Fluxes of sinking particles

The TMF fell within the range of 158–834 mg m^{-2} d^{-1} at a depth of 500 m, 124–628 mg m^{-2} d^{-1} at 1000 m, and 168–1067 mg m^{-2} d^{-1} at 2000 m at the offshore site (Fig. 4; Appendix 1). Furthermore, the TMF was nearly equivalent between 500 and 1000 m (Mann–Whitney *U* test, $P = 0.303$), yielding similar annual TMFs (124 and 112 g m^{-2} yr^{-1}). By contrast, the TMF at 2000 m was 2.5 times higher than at the upper depths, resulting in an annual estimation of 222 g m^{-2} yr^{-1}. The sinking flux of POC fell within the range of 12.1–80.4 mg m^{-2} d^{-1} at 500 m, 11.4–65.2 mg m^{-2} d^{-1} at 1000 m, and 12.3–80.3 mg m^{-2} d^{-1} at 2000 m (Fig. 5A). The sinking flux of PON fell within the range of 1.6–9.3 mg m^{-2} d^{-1} at 500 m, 1.4–7.5 at 1000 m, and 1.4–8.6 at 2000 m (Fig. 5B). The annual POC and PON fluxes were relatively high at 2000 m (14.1 and 1.7 g m^{-2} yr^{-1}, respectively) compared to those at 500 m (10.8 and 1.4 g m^{-2} y^{-1}, respectively) and 1000 m (9.6 and 1.2 g m^{-2} yr^{-1}, respectively). The POC content of the TMF was in the range of 5.8–14.8% at 500 m, 4.6–13.6% at 1000 m, and 4.6–11.6% at 2000 m (Fig. 6A). The PON content was in the range of 0.8–1.8% at 500 m, 0.6–1.6% at 1000 m, and 0.6–1.4% at 2000 m (Fig. 6B). Neither the POC nor the PON content differed between 500 and 1000 m ($P = 0.877$ and 0.273 for C and N, respectively) but both tended to be lower at 2000 m than their equivalent at the upper depths ($P < 0.001$ for four cases).

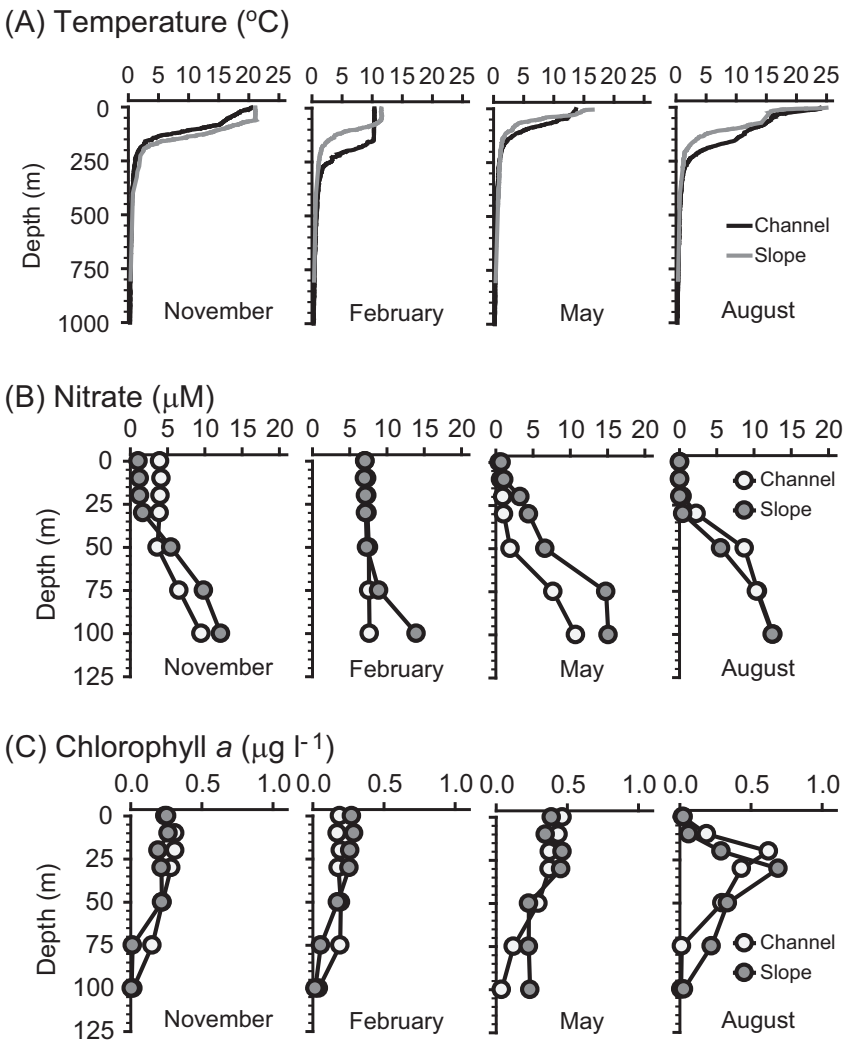

Fig. 3. Vertical profiles of temperature (°C, A), nitrate (μM, B), chlorophyll *a* concentration (μg l^{-1}, C) at the offshore and nearshore sites in February, May, August, and November during the sampling period.

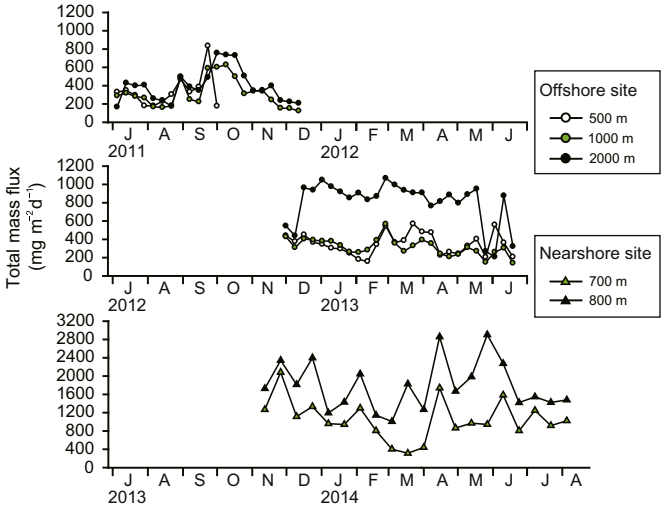

Fig. 4. Time series of the total mass flux (TMF, A), POC flux (B), PON flux (C), carbon content (D), and nitrogen content (E) at; 500, 1000, and 2000 m, at the offshore site from July to December 2011 and from December 2012 to July 2013.

The TMF fell in the range of 315–2086 mg m^{-2} d^{-1} at 700 m and 1009–2905 mg m^{-2} d^{-1} at 800 m at the nearshore site (Fig. 4; Appendix 2). The annual TMF was estimated to be 393 g m^{-2} yr^{-1} at 700 m and 638 g m^{-2} yr^{-1} at 800 m. The sinking flux of POC was in the range of 20.6–109.8 mg m^{-2} d^{-1} at 700 m and 41.3–153.5 mg m^{-2} d^{-1} at 800 m (Fig. 5A). The sinking flux of PON fluctuated within the range of 3.1–13.1 mg m^{-2} d^{-1} at 700 m and 6.8–20.1 mg m^{-2} d^{-1} at 800 m (Fig. 5B). The annual fluxes of POC and PON were estimated to be 23.9 and 3.0 g m^{-2} yr^{-1}, respectively, at 700 m, and 32.1 and 4.5 g m^{-2} yr^{-1}, respectively, at 800 m. The POC and PON contents were slightly higher (P < 0.001 for both cases) at 700 m (4.4–8.3% and 0.5–1.1%, respectively) compared with 800 m (3.1–6.8% and 0.4–1.0%, respectively) (Fig. 6).

3.3. Biogeochemical characteristics of sinking particles

The C/N ratios were lower at 500 m (7.4–10.9; Mann–Whitney U test, P = 0.001 for 500 vs. 1000 m; P < 0.001 for 500 vs. 2000 m) than at 1000 m (7.1–11.6) and 2000 m (8.6–11.6) at the offshore site (Fig. 7A). The C/N range overlapped between 1000 and 2000 m (P = 0.312). The C/N ratio at 700 m (2.4–5.7) was similar to that at 800 m (3.3–6.1; P = 0.043) at the nearshore site. The $\delta^{13}C$ values were lower at 500 m (−22.2‰ to −17.5‰; P < 0.001 for 500 vs. 1000 m; P < 0.001 for 500 vs. 2000 m) than at 1000 m (−21.7‰ to −16.9‰) and

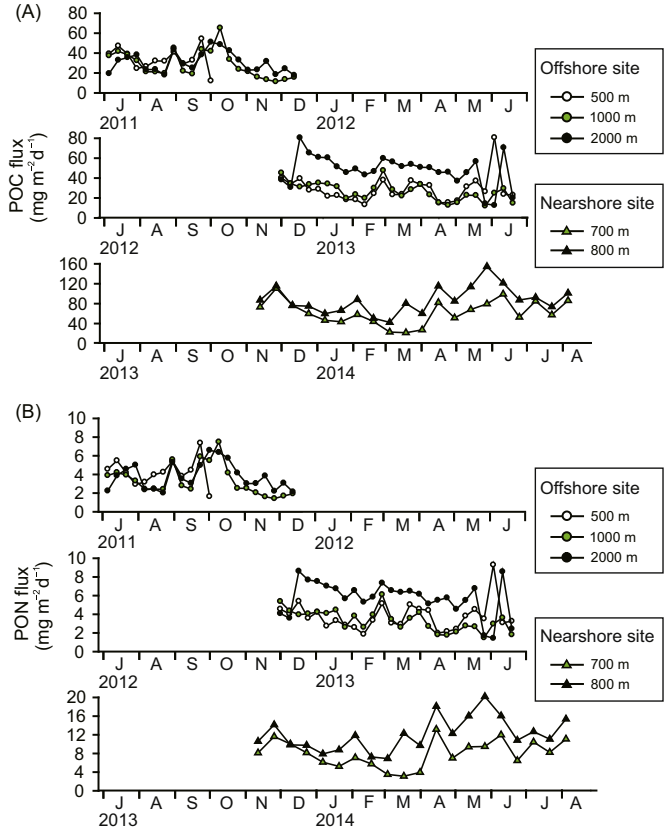

Fig. 5. Time series of the total mass flux (TMF, A), POC flux (B), PON flux (C), carbon content (D), and nitrogen content (E) at; 700 and 800 m, at the nearshore site from November 2013 to August 2014.

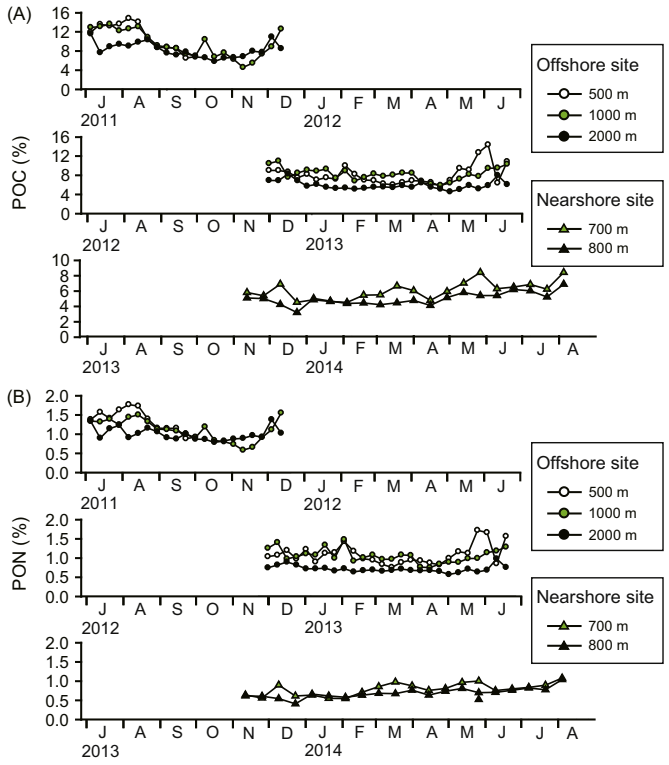

Fig. 6. Variations of C/N ratio (A), $\delta^{13}C$ values (B), and $\delta^{15}N$ values (C) at; 500, 1000, and 2000 m, at the offshore site from July to December 2011 and from December 2012 to July 2013.

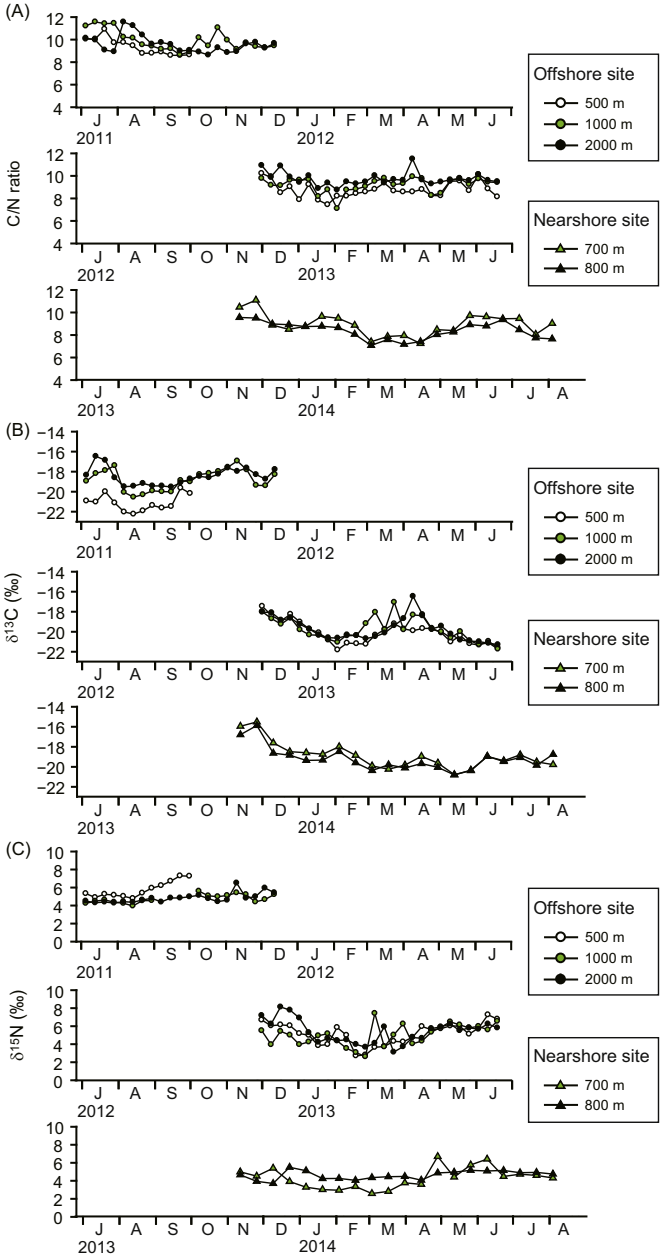

Fig. 7. Variations of C/N ratio (A), $\delta^{13}C$ values (B), and $\delta^{15}N$ values (C) at; 700 and 800 m, at the nearshore site from November 2013 to August 2014.

2000 m (−21.3‰ to −16.5‰) at the offshore site, whereas the values were similar (P = 0.669) between 1000 and 2000 m (Fig. 7B). The $\delta^{13}C$ values were also similar (P = 0.461) between 700 m (−22.6‰ to −15.0‰) and 800 m (−21.2‰ to −17.5‰) at the nearshore site. The $\delta^{15}N$ values were similar at all depths at each site (Kruskal–Wallis test, P = 0.111 for offshore; Mann–Whitney U test, P = 0.192 for nearshore), covering the ranges of 2.6–8.1‰ and 5.0–11.9‰ at the offshore and nearshore sites, respectively (Fig. 7C).

3.4. Temporal patterns of different components and their associations

The TMF (the weighted mean vector was February 22) and fraction of POC (September 22) and PON (September 27) at 2000 m at the offshore site showed unimodal seasonality (Moore's modified Rayleigh test, P < 0.05 for the three cases) (Fig. 8). Axial bimodality (P < 0.05 for the six cases) throughout the year was observed for the temporal distributions of the POC contents (the weighted mean vectors of

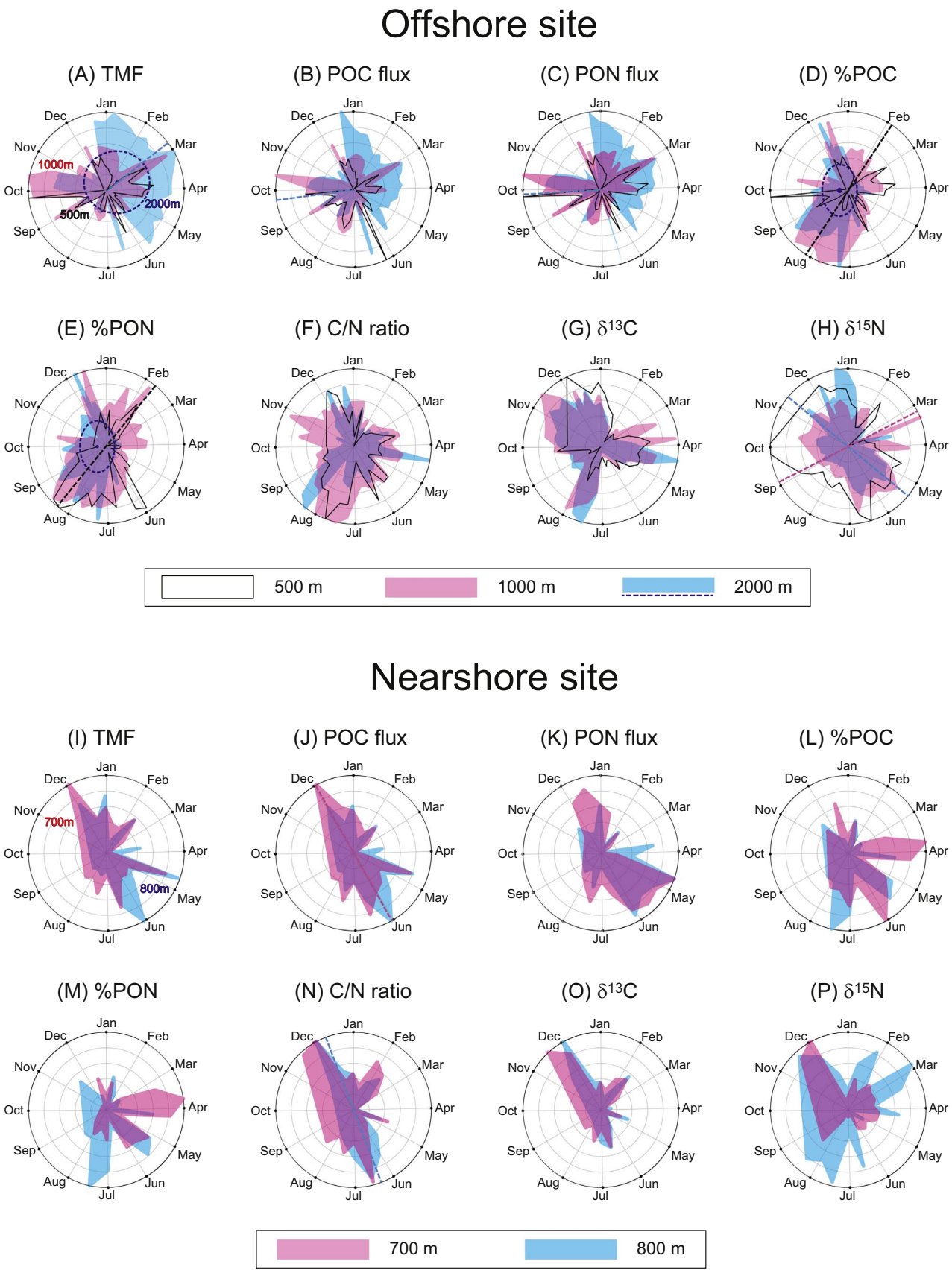

Fig. 8. Polar plots of temporal changes in quantitative and qualitative estimates of sediment trap samples collected at the offshore (A–H) and nearshore (I–P) sites. The estimates were standardized into 0 to 1 scale. The ellipses with broken lines indicate the weighted mean vector standard deviation. The broken lines represent the weighted mean vectors for bimodal or axially bimodal distributions.

February 3 and August 4) and PON (February 9 and August 10) at 500 m and the $\delta^{15}N$ values at 1000 m (March 4 and September 3) and 2000 m (May 11 and November 9) at the offshore site, and the POC content at 700 m (June 1 and December 1) and the C/N ratio at 800 m (June 10 and December 9) at the nearshore site. The other estimates showed random temporal distributions ($P > 0.1$ for unimodality for 37 cases; $P > 0.05$ for bimodality for 34 cases) throughout the year at all depths at both sites without any significant mode (i.e. neither unimodal nor bimodal distributions were found).

Based on Spearman's rank correlation coefficients between the quantitative and qualitative estimates, all quantitative estimates (TMF and fluxes of POC and PON) were positively correlated ($P < 0.05$ for the three cases for each deployment) with each other at all depths at both sites (Appendices 3 and 4). Some quantitative estimates (TMF and POC flux) were positively correlated with qualitative estimates (N content (%), C/N ratios, and $\delta^{13}C$) at the nearshore site ($P < 0.05$ for the six cases for each deployment). By contrast, nonsignificant or weak correlations were found between both estimates at the offshore site.

4. Discussion

This pilot study shows that the annual TMF values and fluxes of POC and PON in the UB of the EJS are high compared with other seas and oceans in the world and other basins in the EJS (Appendix 5). The TMF in the UB (112–638 g m^{-2} yr^{-1}) is much higher than that in the equatorial counter current in the Northwestern Pacific Ocean (2–7 g m^{-2} yr^{-1}, Kempe and Knaack, 1996) and in the Western Pacific subarctic waters and Subarctic Boundary (21–63 g m^{-2} yr^{-1}, Honda et al., 2002). This flux is also higher than that (82–151 g m^{-2} yr^{-1}, Otosaka et al. 2008) in other basins (i.e. Japan and Yamato Basins) of the EJS. In the case of POC in other basins of the EJS, the highest annual flux (11.2 gC m^{-2} yr^{-1}) was reported in the western Japan Basin from 2001 to 2002 and the lowest value (2.0 gC m^{-2} yr^{-1}) was measured in the eastern Japan Basin from 2000 to 2001 (Otosaka et al., 2008). The annual mean flux fell within a range of 0.7–2.8 gC m^{-2} yr^{-1} in the warm waters overwhelmed by the Kuroshio current (Honjo et al., 2008). The annual POC flux of 9.6–32.1 gC m^{-2} yr^{-1} in the present study was remarkably high compared with those in the equatorial counter current in the Northwestern Pacific Ocean (0.1–0.6 g m^{-2} yr^{-1}, Kempe and Knaack, 1996) and in Western subarctic and Subarctic Boundary (0.8–4.3 g m^{-2} yr^{-1}, Honda et al., 2002). The sinking flux of PON in the UB (1.2–4.5 g m^{-2} yr^{-1}) is one order of magnitude higher than those in the Northern Subarctic Pacific seas (0.1–0.15 g m^{-2} yr^{-1}, Wong et al., 1999; Takahashi et al., 2000) and in the South China Sea (0.1–0.3 g m^{-2} yr^{-1}, Chen et al., 1998).

Furthermore, the insignificant temporal distribution of POC indicated that the high annual POC flux was largely sustained by a consistently high POC flux throughout the year rather than by short-term seasonal pulses such as the phytoplankton blooms. The annual POC flux of 10.8 and gC m^{-2} yr^{-1} at 500 m offshore corresponded to 4.0% of the annual primary production (273 gC m^{-2} yr^{-1}; Kwak et al., 2013a). The higher POC flux (23.9 gC m^{-2} yr^{-1}) at 700 m nearshore may result from a higher primary production near the Korean coast (Joo et al., 2014) and lateral transport of re-suspended sediments (Kim et al., 2017). A strong correlation between the quantitative and qualitative estimates further suggested that the increment in TMF in the UB was largely supported by sinking organic debris. By contrast, several estimates of sinking particles had distinct temporal patterns between the bottom depths (2000 m at the offshore site and 800 m at the nearshore site) and their modality was mismatched (Fig. 8). This result indicated that the TMF of the UB might have multiple sources of influence.

One of the most probable explanations for the high annual sinking fluxes in these quantitative estimates is that the primary production was high and persistent throughout the year in the UB (Kwak et al., 2013a, 2014; Joo et al., 2014). Indeed, despite the extremely low chlorophyll *a* concentration of the surface water in August, its summer standing stock (depth-integrated up to 100 m water depth) was comparable to that in May and was higher than that in November and February. The high summer standing stock was likely caused by the maximum in subsurface chlorophyll *a*, which was extensively observed during that time in the basin because of shoaling thermocline and thereby nitracline (Fig. 3; Kwak et al. 2013b; Son et al., 2014). The random distributions of TMF and fluxes of POC and PON in the polar plots indicated significant sinking fluxes even in the well-stratified season (see Figs. 4 and 5). The high POC and PON contents of sinking particles from July to mid-August support the idea that the high sinking fluxes of the quantitative estimates were primarily sustained by export of organic matter from the upper layer during that period (Fig. 6). The synchrony of temporal patterns in quantitative estimates between 500 and 1000 m suggested that the major source of sinking particles might be organic matter from the primary production in the upper euphotic zone (Figs. 4 and 5; Appendix 3). The lowered C/N ratios (close to Redfield ratio of marine phytoplankton-derived debris ≈ 6.6) of sinking particles in late summer also supported this explanation (Fig. 7A). The $\delta^{15}N$ values of the sinking particles falling into the range of nitrate $\delta^{15}N$ values (≈ 4.8‰; Montoya, 2007) confirmed that a large part of the particles comprised organic matter from new production (Fig. 7C). These high summer sinking fluxes reflect well the increased new production of the surface layer (Eppley and Peterson, 1979).

Another possible explanation is that low water temperature (< 1 °C) beneath the 200-m water depth might be responsible for part of the high annual sinking fluxes in the UB. The efficiency of the biological pump is largely controlled by the food web processes of the exported organic matter under the euphotic zone, including ingestion and utilization by microbes and mesozooplankton (Ducklow et al., 2001). In contrast to the consistently high temperature (≈ 13 °C) beneath the 200-m water depth in the Mediterranean Sea, low temperature may reduce the microbial decomposition of organic debris, increasing the efficiency of the biological pump (Fig. 3). The Mediterranean Sea and the EJS constitute almost isolated marginal seas of the eastern and western ends of the Eurasian continent, respectively, at the similar mid-latitude. Despite similar patterns of thermohaline circulation in respective deep basins (Millot and Taupier-Letage, 2005; Lee et al., 2016), these seas display contrasting features in vertical structures of thermal condition and sinking particle flux. In the Mediterranean Sea, the organic carbon flux is reported to be about five times lower at 2000 m than at 200 m, indicating a rapid utilization and/or biodegradation (Marty et al., 1994). In our study sites in the UB, although the POC and PON contents were slightly higher at the upper depths than at the deeper depths, no conspicuous decrease in the absolute values of their contents at the deeper depths was found. Consistent $\delta^{13}C$ and $\delta^{15}N$ values between the upper and deeper depths at both sites might be an indication of a high quantitative contribution of sinking organic flux from the upper to deeper depths. In contrast to the Mediterranean Sea, higher sinking TMF values and fluxes of POC and PON recorded at 2000 m than those at 500 and 1000-m depths of the offshore site in the UB suggest the contribution of particles from lateral transport and sediment resuspension because of relatively strong deep currents (Otosaka et al., 2008; Hyun et al., 2016; Kim et al., 2016a). Despite a possible contribution of these sources to sinking particles, our result further suggested that the uniformly low water temperature below 400 m in the UB might reduce the transformation of the sinking organic debris, probably producing a "refrigerator effect" to conserve sinking organic flux in the water column as speculated by high concentration of dissolved oxygen in the water column and high accumulation rates of labile organic matter in the sediment of the UB (Hyun et al., 2016).

The stable isotope mixing model results in the present study corroborate the high sinking fluxes of total mass and organic matter caused by high primary production in the euphotic zone. We have attempted to assess the relative contribution of intact phytoplankton

aggregations and of zooplankton fecal pellets to sinking particulate material collected in sediment traps by using a stable isotope analysis in R (SIAR; Parnell et al., 2010). SIAR presumes that $\delta^{13}C$ and $\delta^{15}N$ values of the mixture (i.e. sediment trap sample in the present study) falls between those of its potential sources, which differ to each other significantly. The annual mean $\delta^{13}C$ and $\delta^{15}N$ values of phytoplankton and zooplankton fecal pellets were used as end-members of sources in the isotope mixing model. The annual mean $\delta^{13}C$ and $\delta^{15}N$ values were −21.1 and 3.4‰, respectively, for phytoplankton and −20.2 and 8.3‰, respectively, for mesozooplankton. The $\delta^{15}N$ value of zooplankton fecal pellets was estimated by subtracting 1.3‰ from the mesozooplankton value (Altabet and Small, 1990). The isotopic values of the sediment samples at the nearshore sites were within the range of the values of these end-members. Stable isotope mixing model was applied to the sediment samples at the nearshore site, not to those at the offshore site, because the $\delta^{15}N$ values at the offshore sites were lower than the values of the end-members. On the other hand, there are a few limitations of the mixing model estimation in the present study. The difference in the $\delta^{13}C$ values of the end-members was small, broadening the confidence interval. Although multiple sources appear to be included in the sediment trap samples in the UB, we set only two end-members (i.e. intact phytoplankton and mesozooplankton fecal pellets) due to a lack of isotopic data of other potential sources (e.g. microbial decomposer in the water column, benthic microbes and fauna, sediments derived from shelf and slope through lateral advection, and Aeolian input etc.).

The SIAR mixing model estimation indicates that the contribution of intact phytoplankton to sinking organic flux is nearly equal to or slightly higher than that of mesozooplankton fecal pellets (Fig. 9). The higher contribution of intact phytoplankton to the sinking flux in the UB may be explained by high primary production in the euphotic zone as well as the predominance of small copepods, which would inhibit microbial decomposition of sinking particles, in the UB. First, high primary production can result in high proportion of intact phytoplankton in the sediment trap sample because the biomass of phytoplankton relative to that of zooplankton greatly affects the sinking process of organic matter. Sediment traps in high-chlorophyll areas, such as the spring bloom region and the Peru upwelling zone, have historically caught a large amount of intact phytoplankton (Smetacek et al., 1976; Staresinic et al., 1978). In contrast, sediment trap studies in oligotrophic regions reported a high proportion of mesozooplankton fecal pellets and moults (Wiebe et al., 1976; Honjo, 1978; Knauer et al., 1979). High grazing pressure by a large zooplankton population hinders the formation and export of phytoplankton aggregates (e.g. Dubischar and Bathmann, 1997). Furthermore, the species composition of mesozoopankton is also an essential factor determining a major pathway of organic matter export, affecting the contribution of intact phytoplankton to sediment trap sample (Ducklow et al., 2001). Turner (2002) stated that while large fecal pellets of macrozooplankton can constitute an important part of the sedimentary flux, the smaller ones of the micro- and mesozooplankton may be mostly recycled in the water column by microbial decomposition. In fact, the fecal pellets of mesozooplankton account for around one-tenth whereas those of large zooplankton constitute one-third of sinking particles (Wiebe et al. 1979; Madin, 1982; Ducklow et al., 2001). Fecal pellets of small volume typically have a long residence time in the upper water column, which is likely to cause them to be degraded by microbial decomposition and zooplankton coprophages. The dominant zooplankton taxon in the southwestern EJS is small copepods (Ashjian et al., 2005). The fecal pellets of copepods (5 to 220 m d^{-1}) sink slower than those of large species such as euphausiids (16 to 862 m d^{-1}) (Turner, 2002; references therein). As a result, the SIAR estimation in the present study supports that the high fluxes of total mass and organic matters in the UB may result from high primary production of the euphotic zone and the probable low-temperature (i.e., a refrigerator as discussed above) effect in this region.

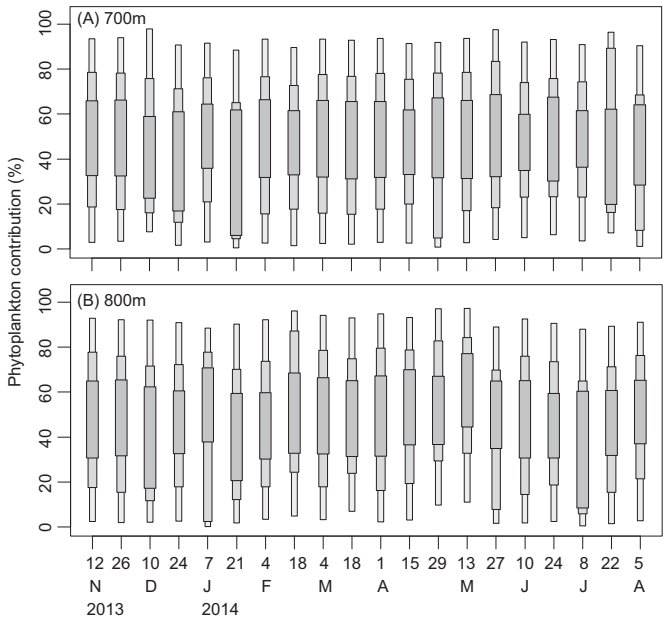

Fig. 9. The relative contribution of intact phytoplankton to the sinking particles (%) compared to that of mesozooplankton fecal pellets (A) at 700 m and (B) at 800 m, at the nearshore site from November 2013 to August 2014.

In summary, the present paper reports preliminary results on vertical fluxes of total mass, POC, and PON for the UB. The annual fluxes corresponded to the upper limit of values reported for other open seas and oceans in the world. No great temporal variability in vertical fluxes was observed, probably reflecting a consistent standing stock of chlorophyll *a* in the upper part of the water column. High contents of POC and PON in sinking particles collected in sediment traps indicated that the primary production in the euphotic zone controls the TMF of the upper layers. The TMF values in the bottom layers were higher than in the upper layers, suggesting a considerable contribution of lateral advection through re-suspended clay mineral to the sedimentary flux (Kim et al., 2017). Along with this allochthonous input, eolian and terrestrial input to the TMF is also expected (Uematsu et al., 1983; Otosaka et al., 2004; Ran et al. 2015), but quantitative estimation of these inputs is beyond the scope of the present study. Based on $\delta^{13}C$ and $\delta^{15}N$ values of phytoplankton, the SIAR mixing model estimation indicated that the significant contribution of intact phytoplankton to sinking organic flux. However, the uncertainties of the isotopic mixing model derived from multiple sources and/or their close isotope values might be resolved by using other biogeochemical tracers such as fatty acids and radioisotopes. Further studies through continuous time-series sediment trap experiments will be essential to better understand the efficiency of the biological carbon pump and the ecological consequences of the climate-induced changes to the pelagic system for the benthic ecosystem in the UB.

Acknowledgements

We would like to thank the captains and crews of R/Vs Onnuri and Tamsa 2. This research was carried out as "Long-term change of structure and function in marine ecosystems of Korea", funded by the Ministry of Oceans and Fisheries, Korea. This study was also partly supported by Korea Institute of Ocean Science and Technology through "Deep-sea Environment & Ecosystem Project of East Sea with Advanced Scientific Technology (PE99399)". Jung Hyun Kwak was supported by Basic Science Research Program through the National Research Foundation of Korea (NRF), funded by the Ministry of Education (NRF-2015R1D1A4A01019937).

Appendix A. Supplementary material

Supplementary data associated with this article can be found in the online version at doi:10.1016/j.dsr2.2017.03.014.

References

Altabet, M.A., Small, L.F., 1990. Nitrogen isotopic ratios in fecal pellets produced by marine zooplankton. Geochim. Cosmochim. Acta 54, 155–163.

Ashjian, C.J., Davis, C.S., Gallager, S.M., Alatalo, P., 2005. Characterization of the zooplankton community, size composition, and distribution in relation to hydrography in the Japan/East Sea. Deep-Sea Res. II 52, 1363–1392.

Ashjian, C.J., Arnone, R., Davis, C.S., Jones, B., Kahru, M., Lee, C., Mitchell, G., 2006. Biological structure and seasonality in the Japan/East Sea. Oceanography 19, 122–133.

Broecker, W.S., 1974. Chemical Oceanography. Harcourt Brace Jovanovich, New York, 214.

Chen, J., Zheng, L., Wiesner, M.G., Chen, R., Zheng, Y., Wong, K.H., 1998. Estimations of primary production and export production in the South China Sea based on sediment trap experiments. Chin. Sci. Bull. 43, 585–586.

Deuser, W.G., 1986. Seasonal and interannual variations in deep-water particle fluxes in the Sargasso Sea and their relation to surface hydrography. Deep-Sea Res. A 33, 225–246.

Deuser, W.G., Ross, E.H., Anderson, R.F., 1981. Seasonality in the supply of sediment to the deep Sargasso Sea and implications for the rapid transfer of matter to the deep ocean. Deep-Sea Res. A 28, 495–505.

Deuser, W.G., Brewer, P.G., Jickells, T.D., Commeau, R.F., 1983. Biological control of the removal of abiogenic particles from the surface ocean. Science 28, 338–391.

Dubischar, C., Bathmann, U.V., 1997. Grazing impact of copepods and salps on phytoplankton in the Atlantic sector of the Southern ocean. Deep-Sea Res. II 44, 415–433.

Ducklow, H.W., Steinberg, D.K., Buesseler, K.O., 2001. Upper ocean carbon export and the biological pump. Oceanography 14 (4), 50–58.

Eppley, R.W., Peterson, B.J., 1979. Particulateorganicmatter flux andplanktonic new production in the deep oceanNature 282, 677–680.

Hahm, D., Kim, K.R., 2001. An estimation of the new production in the southern East Sea using helium isotopes. J. Korean Soc. Oceanogr. 36, 19–26.

Honda, M.C., Imai, K., Nojiri, Y., Hoshi, F., Sugawara, T., Kusakabe, M., 2002. Biological pump in the northwestern North Pacific based on fluxes and major component of particulate matter obtained by sediment trap experiments (1997–2000). Deep-Sea Res. II 49, 5595–5625.

Hong, G.H., Choe, S.-M., Suk, M.-S., 1997a. Annual biogenic particle fluxes to the interior of the East/Japan Sea, a large marginal sea of the Northwest Pacific. In: Tsunogai, S. (Ed.), Biogeochemical Processes in the North Pacific. Japan Marine Science Foundation, Tokyo, 300–321.

Hong, G.H., Kim, S.H., Chung, C.S., 1997b. ^{210}Pb-derived sediment accumulation rates in the southwestern East Sea (Sea of Japan). Geo-Mar. Lett. 17, 126–132.

Hong, G.H., Kim, Y.I., Baskaran, M., 2008. Distribution of ^{210}Po and export of organic carbon from the euphotic zone in the southwestern East Sea (Sea of Japan). J. Oceanogr. 64, 277–292.

Honjo, S., 1978. Sedimentation of materials in the Sargasso Sea at a 5367 m deep station. J. Mar. Res. 36, 469–492.

Honjo, S., Manganini, S.J., Krishfield, R.A., Francois, R., 2008. Particulate organic carbon fluxes to the ocean interior and factors controlling the biological pump: a synthesis of global sediment trap programs since 1983. Prog. Oceanogr. 76, 217–285.

Hyun, J.-H., 2016. Microbial ecology and biogeochemical processes in the Ulleung Basin. In: Chang, K.-I. (Ed.), Oceanography of the East Sea (Japan Sea). Springer International Publishing, Cham, 247–296.

Hyun, J.H., Kim, D., Shin, C.W., Noh, J.H., Yang, E.J., Mok, J.S., Kim, S.H., Kim, H.C., Yoo, S., 2009. Enhanced phytoplankton and bacterioplankton production coupled to coastal upwelling and ananticyclonic eddy in the Ulleung Basin. East Sea. Aquat. Microb. Ecol. 54, 45–54.

Iversen, M.H., Nowald, N., Ploug, H., Jackson, G.A., Fischer, G., 2010. High resolution profiles of vertical particulate organic matter export off Cape Blanc, Mauritania: degradation processes and ballasting effectsDeep-Sea Res. I 57, 771–784.

Joo, H.T., Park, J.W., Son, S.H., Noh, J.-H., Jeong, J.-Y., Kwak, J.H., Saux-Picart, S., Choi, J.H., Kang, C.K., Lee, S.H., 2014. Long-term annual primary production in the Ulleung Basin as a biological hot spot in the East/Japan Sea. J. Geophys. Res. Ocean. 119, 3002–3011.

Karl, D.M., Christian, J.R., Dore, J.E., Hebel, D.V., 1996. Seasonal and interannual variability in primary production and particle flux at Station ALOHA. Deep-Sea Res. II 43, 539–568.

Kempe, S., Knaack, H., 1996. Vertical particle flux in the western Pacific below the north Equatorial Current and the Equatorial Counter Current. In: Ittekkot, V., Schäfer, P., Honjo, S., Depetris, P.J. (Eds.), Particle Flux in the Ocean. John Wiley and Sons, New York, 313–323.

Kim, D., Choi, M.S., Oh, H.Y., 2011. Seasonal export fluxes of particulate organic carbon from ^{234}Th/^{238}U disequilibrium measurements in the Ulleung basin (Tsushima basin) of the East Sea (Sea of Japan). J. Oceanogr. 67, 577–588.

Kim, I.-N., Lee, K., Hwang, J., 2016a. Natural and anthropogenic carbon cycling. In: Chang, K.-I. (Ed.), Oceanography of the East Sea (Japan Sea). Springer International Publishing, Cham, 169–189.

Kim, K., Kim, K.R., Min, D.H., Volkov, Y., Yoon, J.H., Takematsu, M., 2001. Warming and structural changes in the East (Japan) Sea: a clue to future changes in global oceans? Geophys. Res. Lett. 28, 3293–3296.

Kim, M., Hwang, J., Rho, T.K., Lee, T., Kang, D.J., Chang, K.-I., Noh, S., Joo, H.T., Kwak, J.H., Kang, C.K., Kim, K.-R., 2017. Biogeochemical properties of sinking particles in the southwestern part of the East Sea (Japan Sea). J. Mar. Syst. 167, 33–42.

Knauer, G.A., Martin, J.H., Bruland, K.W., 1979. Fluxes of particulate carbon, nitrogen, and phosphorus in the upper water column of the northeast Pacific. Deep-Sea Res. A 26, 97–108.

Kovach, W.L., 1994. Oriana for Windows, Ver. 1.0. Kovach cOmputing Services. Pentraeth, Wales, United Kingdom.

Kwak, J.H., Lee, S.H., Park, H.J., Choy, E.J., Jeong, H.D., Kim, K.R., Kang, C.K., 2013a. Monthly measured primary and new productivities in the Ulleung Basin as a biological "hot spot" in the East/Japan Sea. Biogeosciences 10, 4405–4417.

Kwak, J.H., Hwang, J., Choy, E.J., Park, H.J., Kang, D.-J., Lee, T., Chang, K.-I., Kim, K.-R., Kang, C.K., 2013b. High primary productivity and f-ratio in summer in the Ulleung Basin of the East/Japan Sea. Deep-Sea Res. I 79, 74–85.

Kwak, J.H., Lee, S.H., Hwang, J., Suh, Y.-S., Park, H.J., Chang, K.-I., Kim, K.-R., Kang, C.K., 2014. Summer primary productivity and phytoplankton community composition driven by different hydrographic structures in the East/Japan Sea and the Western Subarctic Pacific. J. Geophys. Res. Ocean. 119, 45054–45519.

Laurenceau-Cornec, E.C., Trull, T.W., Davies, D.M., Bray, S.G., Doran, J., Planchon, F., Carlotti, F., Jouandet, M.-P., Cavagna, A.-J., Waite, A.M., Blain, S., 2015. The relative importance of phytoplankton aggregates and zooplankton fecal pellets to carbon export: insights from free-drifting sediment trap deployments in naturally iron-fertilised waters near the Kerguelen Plateau. Biogeosciences 12, 1007–1027.

Lee, J.Y., Kang, D.J., Kim, I.N., Rho, T., Lee, T., Kang, C.K., Kim, K.R., 2009. Spatial and temporal variability in the pelagic ecosystem of the East Sea (Sea of Japan): a review. J. Mar. Syst. 78, 288–300.

Lee, D.-K., Seung, Y.H., Kim, Y.-B., Kim, Y.H., Shin, H.-R., Shin, C.-W., Chang, K.-I., 2016. Circulation. In: Chang, K.-I. (Ed.), Oceanography of the East Sea (Japan Sea). Springer International Publishing, Cham, 87–126.

Madin, L.P., 1982. Production, composition and sedimentation of salp fecal pellets in oceanic waters. Mar. Biol. 67, 39–45.

Marty, J.C., Nicolas, E., Miquel, J.C., Fowler, S.W., 1994. Particulate fluxes of organic compounds and their relationship to zooplankton fecal pellets in the northwestern Mediterranean Sea. Mar. Chem. 46, 387–405.

McCave, I.N., 1975. Vertical flux of particles in the ocean. Deep Sea Res. Oceanogr., 7.

Millot, C., Taupier-Letage, I., 2005. Circulation in the Mediterranean Sea. In: Saliot, A. (Ed.), Handbook of Environmental Chemistry 5. Springer, New York, 29–66.

Mohiuddin, M.M., Nishimura, A., Tanaka, Y., Shimamoto, A., 2004. Seasonality of biogenic particle and planktonic foraminifera fluxes: response to hydrographic variability in the Kuroshio Extension, northwestern Pacific Ocean. Deep-Sea Res. I 51, 1659–1683.

Montoya, J.P., 2007. Natural abundance of ^{15}N in marine planktonic ecosystems. In: Michener, R., Lajtha, K. (Eds.), Stable Isotopes in Ecology and Environmental Sciencesecond ed. Blackwell Publisher, Oxford, 176–201.

Osterbererg, B., Carey, A.G., Curl, H., 1963. Acceleration of sinking rates of radionucliders in the ocean. Nature 200, 1276–1277.

Otosaka, S., Togawa, O., Baba, M., Karasev, E., Volkov, Y.N., Omata, N., Noriki, S., 2004. Lithogenic flux in the Japan Sea measured with sediment traps. Mar. Chem. 91, 143–163.

Otosaka, S., Tanaka, T., Togawa, O., Amano, H., Karasev, E.V., Minakawa, M., Noriki, S., 2008. Deep sea circulation of particulate organic carbon in the Japan Sea. J. Oceanogr. 64, 911–923.

Parnell, A.C., Inger, R., Bearhop, S., Jackson, A.L., 2010. Source partitioning using stable isotope: coping with too much variation. PLoS One 5 (3), e9672. http://dx.doi.org/10.1371/journal.pone.0009672.

Parsons, T.R., Maita, Y., Lalli, C.M., 1984. A Manual of Chemical and Biological Methods for Seawater and Analysis.. Pergamon Press, Oxford, 173.

Ran, L., Chen, J., Wiesner, M.G., Ling, Z., Lahajnar, N., Yang, Z., Li, H., Hao, Q., Wang, K., 2015. Variability in the abundance and species composition of diatoms in sinking particles in the northern South China Sea: results from time-series moored sediment traps. Deep-Sea Res. II 122, 15–24.

Smetacek, V., von Bodungen, B., von Bröckel, K., Zeitzschel, B., 1976. The plankton tower. II. Release of nutrients from sediments due to changes in the density of bottom water. Mar. Biol. 34, 373–378.

Son, Y.-T., Chang, K.-I., Yoon, S.-T., Rho, T., Kwak, J.H., Kang, C.K., Kim, K.-R., 2014. A newly observed physical cause of the onset of the subsurface spring phytoplankton bloom in the southwestern East Sea/Sea of Japan. Biogeosciences 11, 1319–1329.

Staresinic, N., Rowe, G.T., Shaughnessey, D., Williams, A.J., III, 1978. Measurement of the vertical flux of particulate organic matter with a free-drifting sediment trap. Limnol. Oceanogr. 23, 559–563.

Takahashi, K., Fujitani, N., Yanada, M., Maita, Y., 2000. Long-term biogenic particle fluxes in the Bering Sea and the central subarctic Pacific Ocean, 1990–1995. Deep-Sea Res. I 47, 1723–1759.

Talley, L.D., Min, D.H., Lobanov, V.B., 2006. Japan/East Sea water masses and their relation to the sea's circulation. Oceanography 19, 32–49.

Thunell, R.C., 1998. Seasonal and annual variability in particle fluxes in the Gulf of California: a response to climate forcing. Deep-Sea Res. I 45, 2059–2083.

Turner, J.T., 2002. Zooplankton fecal pellets, marine snow and sinking phytoplankton blooms. Aquat. Microb. Ecol. 27, 57–102.

Uematsu, M., Duce, R.A., Prospero, J.M., Chen, L., Merrill, J.T., McDonald, R.L., 1983. Transport of mineral aerosol from Asia over the North Pacific Ocean. J. Geophys. Res. 88, 5343–5352.

Volk, T., Hoffert, M.I., 1985. Ocean carbon pumps: analysis of relative strength and efficiencies of in ocean-driven circulation atmospheric CO_2 changes. In: Sundquist,

E.T., Broecker, W.S. (Eds.), The Carbon Cycle and Atmospheric CO_2: Natural Variation Archean to Present: AGU Monograph 32. American Geophysical Union, Washington, DC, 99–110.
Wiebe, P.H., Boyd, S.H., Winget, C.L., 1976. Particulate matter sinking to the deep-sea floor at 2000 m in the Tongue of the Ocean, Bahamas, with a description of a new sedimentation trap. J. Mar. Res. 34, 341–354.
Wiebe, P.H., Madin, L., Haury, L., Harbison, G.R., Philbin, L., 1979. Diel vertical migration by salpa-aspera and its potential for largescale particulate organic matter transport to the deep-sea. Mar. Biol. 53, 249–255.
Wong, C.S., Whitney, F.A., Crawford, D.W., Iseki, K., Matear, R.J., Johnson, W.K., Page, J.S., Timothy, D., 1999. Seasonal and interannual variability in particle fluxes of carbon, nitrogen and silicon from time series of sediment traps at Ocean Station P, 1982–1993: relationship to changes in subarctic primary productivity. Deep-Sea Res. II 46, 2735–2760.
Yamada, K., Ishizaka, J., Nagata, H., 2005. Spatial and temporal variability of satellite primary production in the Japan Sea from 1998 to 2002. J. Oceanogr. 61, 857–869.
Yoo, S., Park, J., 2009. Why is the southwest the most productive region of the East Sea/Sea of Japan? J. Mar. Syst. 78, 301–315.
Zar, J.H., 1998. Biostatistical analysis. Upper Saddle River: Prentice Hall, NJ.